JOURNAL OF Materials CHEMISTRY

Hydrotalcites as sorbent for 2,4,6-trinitrophenol: influence of the layer composition and interlayer anion

C. Barriga,[a] M. Gaitán,[a] I. Pavlovic,[a] M. A. Ulibarri,*[a] M. C. Hermosïn[b] and J. Cornejo[b]

[a]*Departamento de Química Inorgánica e Ingeniería Química. Campus Universitario Rabanales, Edificio C3, 1ª Planta. Universidad de Córdoba, Córdoba 14071, Spain. E-mail: iq1ulcom@uco.es*
[b]*Instituto de Recursos Naturales y Agrobiología de Sevilla.CSIC, Sevilla, Spain*

Received 3rd September 2001, Accepted 17th December 2001
First published as an Advance Article on the web 8th February 2002

This work evaluates the effects of different variables such as M^{II}/M^{III} ratio (layer charge), interlayer anion (CO_3^{2-} or Cl^-) and nature of the trivalent cation (Al^{3+} or Fe^{3+}) in the sorption of 2,4,6-trinitrophenol (TNP) by layered double hydroxides (LDH) $[M^{II}_{1-x}M^{III}_x(OH)_2]A^{n-}_{x/n}\cdot mH_2O$ ($M^{II} = Mg^{2+}$, $M^{III} = Al^{3+}$ or Fe^{3+}, $A = CO_3^{2-}$ or Cl^-, $x = 0.33 - 0.20$) and its calcined products $M^{II}_{1-x}M^{III}_xO_{1+x/2}$. TNP adsorption by anionic exchange is strongly affected by exchangeable interlayer anion, being dramatically favoured in the case of MgAlCl. TNP adsorption by anionic exchange on the $MgAlCO_3$ system is very low and it is not affected by the Mg/Al ratio while it is in MgAlCl. In the case of the MgFeCl system, the higher polarizing character of Fe^{3+} makes the exchange reaction less favorable. TNP adsorption by reconstruction of the calcined products decreases in the order $MgAlCO_3500 >$ MgAlCl500 $>$ MgFeCl500, and it is favored by the layer charge decrease.

Introduction

Layered double hydroxides (LDH) constitute an interesting class of layered compounds, also called hydrotalcites and anionic clays.[1–4] Their general formula may be represented as $[M^{II}_{1-x}M^{III}_x(OH)_2]A^{n-}_{x/n}\cdot mH_2O$. The structure is derived from that of brucite, $Mg(OH)_2$, *i.e.* a hexagonal close-packing of hydroxide ions, with all octahedral sites every two layers occupied by M(II) and M(III) ions. Partial substitution of M(III) for M(II) gives rise to positively charged layers thus leading to location of anions in unoccupied interlayers. Water molecules also exist in the interlayer space. A schematic representation of the structure is shown in Fig. 1. The interlayer anions can be easily exchanged[5] and a wide variety of inorganic and organic anions can be present in the interlayer.[6–8] The nature of the layer cations can be also diverse including transition metal cations.[8–12] Calcination of LDH produces intermediate non-stoichiometric oxides[13–16] which undergo rehydration in aqueous medium and regain the hydroxide structure with different anions in the interlayer.[17–19]

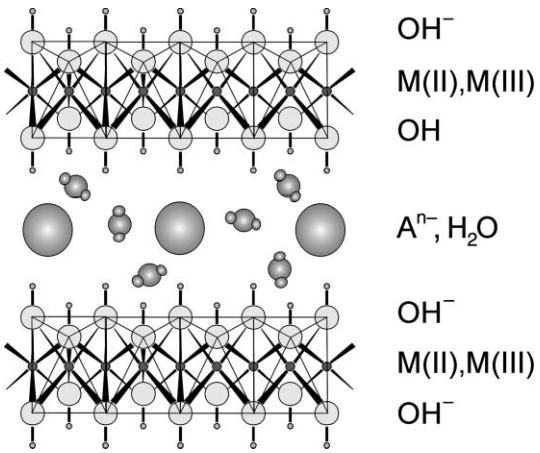

Fig. 1 Schematic representation of the hydrotalcite-like structure.

Most applications of LDH correspond to the field of heterogeneous catalysis[20–24] but they also attract attention as ion exchangers, molecular sieves, protonic conductors, PVC stabilizers, antiacids (medicine), wastewater treatments, *etc.*[25]

The development of new sorbents with application in water decontamination is a research topic of maximum interest and in this field clay minerals and organoclays have been widely studied for removing polar and non-polar contaminants.[26–31] The anionic clays, as antagonist of clay minerals, offer a large interlayer surface to host diverse anionic species[2,4] with the additional advantage that they can be easily recycled.[32] LDH and their calcined products have been shown to be good sorbents for organic anionic contaminants likely to be found in residual waters, such as phenols, surfactants, pesticides, *etc.*, which adsorb by anionic exchange or reconstruction in the layered structure.[33–36] This sorption process must be affected by the composition of the hydrotalcite, which determines the layer charge, the nature of the anion present in the interlayer and the nature of the metal ions in the layer. These characteristics determine the accessibility of the anionic interlayer positions and hence should influence the adsorption of the anionic contaminants in these type of sorbents.

This work deals with studying the effect of the above mentioned variables: M^{II}/M^{III} ratio or layer charge, the interlayer anion (CO_3^{2-} or Cl^-) and the nature of the trivalent cation (Al^{3+} or Fe^{3+}), in the sorption of 2,4,6-trinitrophenol (TNP, $pK_a = 0.38$), selected as a model for the anionic organic contaminant. The results of this work could help to optimize and rationalize the design of structural properties of the appropriate sorbent.

Materials and methods

Sorbent synthesis

LDH with carbonate and chloride in the interlayer and Mg–Al in the layer (Mg^{II}/Al^{III} molar ratios 4, 3 and 2) and Mg–Fe–Cl ($Mg^{II}/Fe^{III} = 3$) have been prepared by the coprecipitation method.[2]

a) Carbonate-containing Mg–Al LDH. Two solutions containing $Mg(NO_3)_2{\cdot}6H_2O$ and $Al(NO_3)_3{\cdot}9H_2O$ with Mg/Al ratio = 4, 3 and 2, $[Mg^{II} + Al^{III}] = 0.24$ moles in 500 ml of distilled water, and 0.6 mol NaOH in 100 ml of water, respectively, were added with vigorous stirring to a solution containing 0.033 mol Na_2CO_3 in 100 ml of water. The resulting slurry was aged for 60 h and dried at 60 °C for 24 h.

b) Chloride-containing Mg–Al and Mg–Fe LDH. A solution containing 0.5 mol NaOH in 250 ml of distilled and boiled water was added to a solution containing 0.18 mol $MgCl_2{\cdot}6H_2O$ and 0.06 mol $AlCl_3{\cdot}6H_2O$ or $FeCl_3{\cdot}6H_2O$ in 500 ml of water, maintaining the pH at 10. During addition, nitrogen was bubbled through the suspension. The products were subjected to hydrothermal treatment at 120 °C for 72 h, washed with carbonate-free water and dried at 80 °C for 24 h. Samples with ratio Mg/Al = 4 and 2 have been prepared by the same method.

c) Calcined products. The carbonate and chloride LDH with Mg/Al = 4, 3, and 2 and chloride LDH with Mg/Fe = 3 were calcined at 500 °C during 24 h to prepare the mixed oxides

The carbonate and chloride samples are designated $XM^{II}M^{III}Y$ where X stands for nominal M^{II}/M^{III} atomic ratio and Y for interlayer anion, and $XM^{II}M^{III}Y500$ for calcined products.

Sorbent characterization

Mg, Al, Fe elemental chemical analyses were obtained using atomic absorption spectroscopy after dissolution of solid in 0.1 M HCl (Perkin Elmer model 3100). Powder X-ray diffraction (PXRD) patterns were recorded with a Siemens D500 instrument, with Ni-filtered Cu-K_α radiation, using steps of 0.02° (2θ) and a time constant of 0.6 s. IR spectra were obtained on a FT-IR Nicolet 510P spectrophotometer with the samples diluted as KBr disks. Microstructural characterization of the material was carried out using a JEOL 200CX TEM.

Adsorption experiments

The TNP adsorption on $XM^{II}M^{III}Y$ and $XM^{II}M^{III}Y500$ was measured by batch equilibration techniques at diverse initial phenol concentrations from 1 to 50 mM (adsorption isotherms) as reported elsewhere.[32,34] The suspensions (sorbent and TNP aqueous solution) were shaken at room temperature and after adequate time (2 h for original hydrotalcites and 24 h for calcined samples) previously determined,[34] the supernatants were filtered to determine the contaminant concentration by UV absorbance at 360 nm. The spectrophotometric measurements were recorded using a Perkin-Elmer model Lambda 11 UV–visible spectrophotometer. The amounts adsorbed were determined from the initial (C_i) and final or equilibrium (C_e) concentration of the contaminant solution. The adsorption isotherms were described quantitatively by application of the Langmuir equation:[37]

$$C_e/C_s = (C_e/C_m) + (1/C_mL) \quad (3)$$

where C_e is the solute (adsorbate) concentration in the solution at equilibrium (μmol ml^{-1}), C_s the amount of solute adsorbed in the solid at equilibrium (μmol g^{-1}), C_m the maximum adsorption capacity at a monolayer coverage (μmol g^{-1}) and L is a constant related to the adsorption energy.

Synthesis of LDH–TNP

In order to obtain the total anionic exchange product, LDH–TNP, with TNP as unique interlayer anion, two methods of synthesis were used: a) anionic exchange by treatment of $XM^{II}M^{III}Y$ with 40 mM TNP solution at pH = 2 and pH = 6 for $3MgAlCO_3$ and 3MgFeCl samples, respectively, by stirring during 24 h and b) reconstruction of $3MgAlCO_3500$ and 3MgFeCl500 with 40 mM TNP solution at pH = 4 under CO_2 free conditions. The LDH–TNP products thus obtained were identified by X-ray diffraction and FT-IR spectroscopy.

Results and discussion

Characterization of the sorbents

The sorbents were characterized by X-ray diffraction, FT-IR spectroscopy and TEM. Some characteristics are summarized in Table 1. Mg, Al and Fe were determined by elemental chemical analyses and according to the results, the M^{II}/M^{III} atomic ratios in coprecipitated solid (chloride and carbonate) are close to the theoretical values, Table 1.

The XRD patterns for all samples are characteristic of layered materials with hydrotalcite like structure. Some selected patterns, $3MgAlCO_3$ and 3MgFeCl, are included in Fig. 2. The a lattice parameter shows an increase from 3.04 Å for ratio Mg/Al = 2 to 3.06 for Mg/Al = 4 due to the larger ionic radius of Mg^{II} (0.86 Å) than Al^{III} (0.67 Å) in octahedral coordination (Table 1). The substitution of the trivalent cation produces an increase from 3.05 Å for 3MgAlCl to 3.10 Å for 3MgFeCl (ionic radius of Fe^{III} is 0.78 Å). Consistently the value of lattice parameter c decreases as charge density increases due to the electrostatic attraction between the positive sheets and the anions in the interlayer. The value of c is also a function of the nature of the interlayer anions and of the hydration state.[2] According to the size and charge of the interlayer anion an increase in the c parameter is observed for Cl^- *versus* CO_3^{2-}. The values are also included in Table 1.

The XRD patterns of the calcined products $3MgAlCO_3500$ and 3MgFeCl500 are shown in Fig. 2b and d. The calcination of $3MgAlCO_3$ at 500 °C results in collapse of the hydrotalcite structure.[2] Fig. 2b shows only two broad peaks (d = 2.08 Å and d = 1.48 Å), which correspond to the (200) and (220) diffraction lines of the MgO cubic phase ($Fm3m$). However this pattern was shifted to a higher position of 2θ, indicating that the substitution of Al^{3+}, with a smaller ion radius, into MgO, occurred at 500 °C to form a solid solution of ideal composition $Mg_6Al_2O_9$.[38] Lines corresponding to the formation of the spinel $MgAl_2O_4$ are not present (Fig. 2b). However, the XRD lines corresponding to the spinel $MgFe_2O_4$ were detected, in addition to those of MgO, in the calcined product 3MgFeCl500 at the same temperature (500 °C) (Fig. 2d).

The XRD pattern of 3MgFeCl500 shows the main lines of the $MgFe_2O_4$ (2.52, 2.10, 1.61 and 1.48 Å) and MgO phases (2.10 and 1.41 Å). However, the relative intensities of lines corresponding to this pattern appear modified because the mixture of both phases with cubic symmetry produces diffraction at the same values of 2θ. The line at 2.52 Å corresponds only to the $MgFe_2O_4$ phase but the line at 2.10 Å corresponds to both phases.

FT-IR spectra of samples $3MgAlCO_3$ (Fig. 3a) and

Table 1 Characteristics of the hydrotalcite prepared

Sample	Formula[a]	a/Å[b]	c/Å[b]	AEC[c]
$2MgAlCO_3$	$[Mg_{4.14}Al_{1.86}(OH)_{12}](CO_3)_{0.93}{\cdot}nH_2O$	3.04_2	22.83	4023
$3MgAlCO_3$	$[Mg_{5.84}Al_{2.16}(OH)_{16}](CO_3)_{1.08}{\cdot}nH_2O$	3.05_3	23.22	3312
$4MgAlCO_3$	$[Mg_{7.97}Al_{2.03}(OH)_{20}](CO_3)_{1.02}{\cdot}nH_2O$	3.06_1	23.32	2712
2MgAlCl	$[Mg_{4.2}Al_{1.8}(OH)_{12}]Cl_{1.8}{\cdot}nH_2O$	3.04_8	23.36	4014
3MgAlCl	$[Mg_{6.08}Al_{1.92}(OH)_{16}]Cl_{1.92}{\cdot}nH_2O$	3.05_4	23.56	3253
4MgAlCl	$[Mg_{8.1}Al_{1.94}(OH)_{20}]Cl_{1.94}{\cdot}nH_2O$	3.06_8	23.76	2734
3MgFeCl	$[Mg_{5.96}\ Fe_{2.04}(OH)_{16}]Cl_{2.04}{\cdot}nH_2O$	3.10_4	24.09	2974

[a]Obtained by absorption atomic spectroscopy data. [b]a and c lattice parameters. [c]Anionic exchange capacity (μmol g^{-1}) calculated from theoretical formula $[M^{II}_{1-x}M^{III}_x(OH)_2]A^{n-}_{x/n}{\cdot}mH_2O$ with M^{II}/M^{III} = 2, 3 and 4.

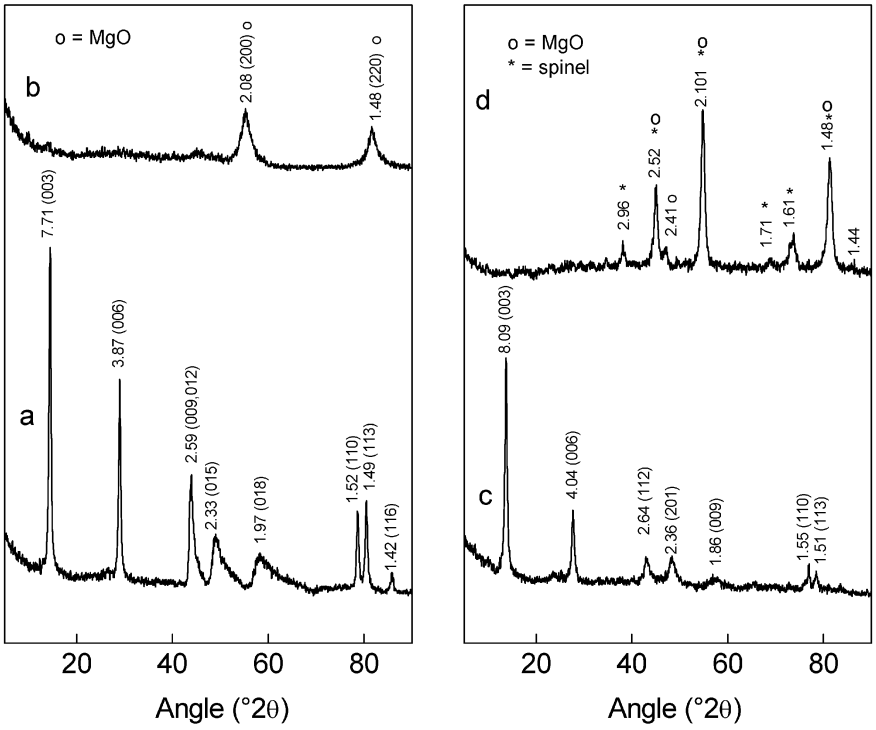

Fig. 2 X-Ray diffraction patterns of a) $3MgAlCO_3$, b) $3MgAlCO_3500$, c) 3MgFeCl and d) 3MgFeCl500.

3MgAlCl (Fig. 3b) differ only in the bands attributed to the interlayer anion. The broad absorption peak in both spectra between 3600 and 3300 cm^{-1} is due to the ν(OH) mode of the hydroxy groups, both from the brucite-like layers and from interlayer water molecules. Interlayer water also gives rise to the broad, medium-intensity, absorption close to 1630 cm^{-1}, $\delta(H_2O)$. Hydrogen bonding of the water with interlayer carbonate anions also gives rise to a shoulder at 3064 cm^{-1} in the spectrum of sample $3MgAlCO_3$.[39,40] The very intense absorption band at 1361 cm^{-1} in the spectrum 3a corresponds to the ν_3 mode of the carbonate species. Absorptions below 800 cm^{-1} are due to lattice vibrations, involving metal–oxygen stretching modes and, in the case of the sample $3MgAlCO_3$, also modes ν_2 (out-of-plane deformation) and ν_4 (in-plane bending) of carbonate at 864 and 670 cm^{-1}, respectively. The FT-IR spectrum of the sample 3MgFeCl (not shown) was analogous to those of 3MgAlCl.

FT-IR spectra of all calcined products were similar, and two of them are shown in Fig. 3c and d ($3MgAlCO_3500$ and 3MgFeCl500 respectively). Spectra suggest that some

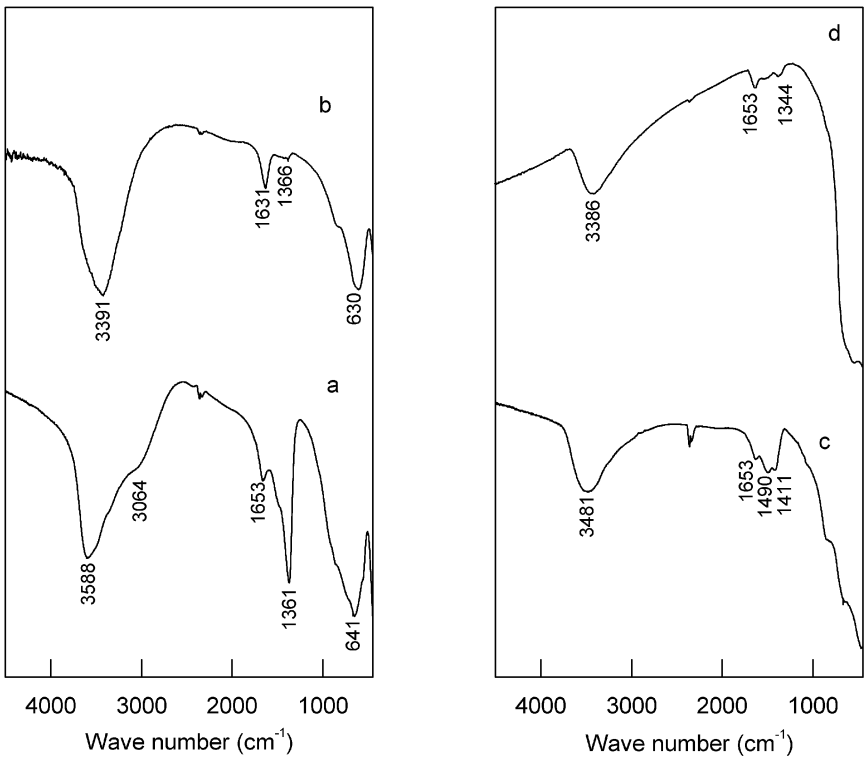

Fig. 3 FT-Infrared spectra a) $3MgAlCO_3$, b) 3MgAlCl, c) $3MgAlCO_3500$ and d) 3MgFeCl500.

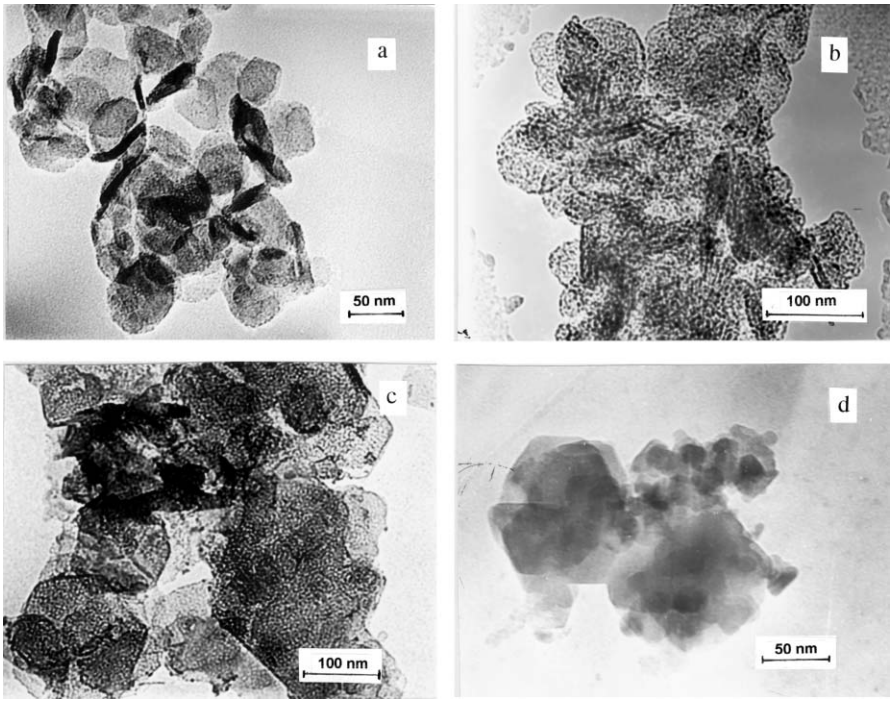

Fig. 4 TEM micrograph of a) $3MgAlCO_3$ b) $3MgAlCO_3500$ c) 3MgFeCl and d) 3MgFeCl500.

carbonate anions are present in both samples (bands at 1411 cm^{-1} for 3MgAlCl500 and 1379 cm^{-1} from 3MgFeCl500). From the low intensity of these peaks relative to the corresponding one in the spectrum of $3MgAlCO_3$ it is inferred that the amount of carbonate is considerably less. Therefore, the IR bands assigned to carbonate stretches on these calcined samples could be due to some carbonate species adsorbed on the surface.

TEM micrographs for selected samples are shown in Fig. 4. Plate-like particles with hexagonal morphology are observed for all samples. The medium size of the particles for $3MgAlCO_3$ was *ca.* 50 nm. The electron micrograph of calcined product $3MgAlCO_3500$ shows the particles maintaining the external shape but a noticeable network of cracks appears in the surface. The thermal decomposition process induces the occurrence of pores because of the escape of CO_2 and H_2O gases through the particles.[9] However, the calcined product of sample 3MgFeCl500 shows a hexagonal morphology with smooth surfaces and there are no differences of contrast produced by the porous system. In the last case the product contains two phases and higher crystallinity than $3MgAlCO_3500$ (see XRD pattern, Fig. 2d). The particle size did not show any regularity in this case.

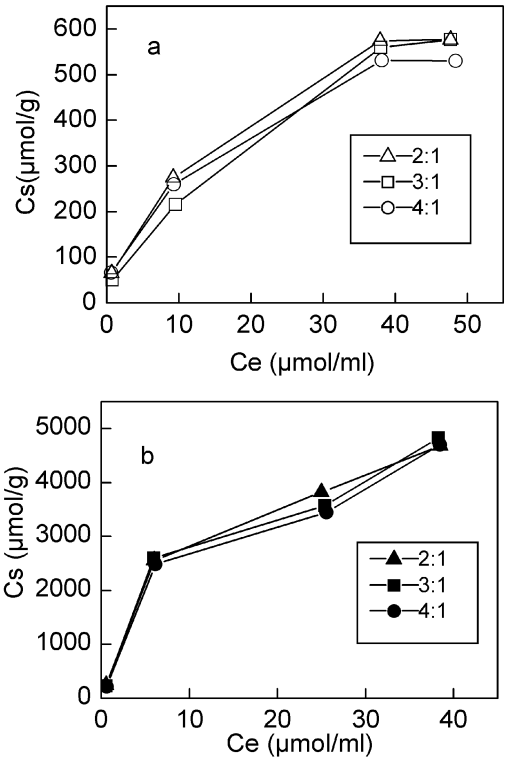

Fig. 5 Adsorption isotherms of TNP on different sorbents. a) XMgAlCO$_3$, pH = 2, 0.05 g of sorbent per 10 ml of TNP, 2 h, b) XMgAlCO$_3$500, 0.05 g of sorbent per 10 ml of TNP pH = 4, 2 h.

Adsorption results

$MgAlCO_3$ system. *Influence of the layer charge (Mg/Al ratio).* The TNP adsorption isotherms on XMgAlCO$_3$, with layers of different charge are shown in Fig. 5a. The adsorption isotherms were all of the L-type according to the classification of Giles *et al.*,[41] indicating a system where monofunctional molecules or ions adsorb on specific sites of the sorbent, mostly by ion–ion interaction and reaching a saturation value given by the "plateau" of the adsorption isotherm. The values of the maximum adsorption were quantitatively described by the application of the Langmuir equation, and are given in Table 2. C_m represents the maximum sorption capacity, and for L-type isotherms this value coincides with the "plateau", and L is a

Table 2 Langmuir model parameters for TNP adsorption and the corresponding %AEC of XMgAlCO$_3$ (X = 2, 3 and 4) hydrotalcite compounds and their calcined products (XMgAlCO$_3$500)[a]

Adsorbent	C_m/μmol g^{-1}	L	r^2	%AEC
$2MgAlCO_3$ pH = 2	699	0.100	0.99	17
$3MgAlCO_3$ pH = 2	566	0.024	0.99	17
$4MgAlCO_3$ pH = 2	526	0.172	0.98	19
$2MgAlCO_3$500 pH = 4	5880	0.094	0.98	77
$3MgAlCO_3$ 500 pH = 4	6250	0.070	0.97	>100
$4MgAlCO_3$500 pH = 4	5882	0.073	0.97	>100

[a]AEC XMgAlCO$_3$500 = 7598, 5817 and 4714 μmol g^{-1} for X = 2, 3 and 4, respectively.

constant related to the adsorption energy.[37] According to the data in Table 2, the exchange process of TNP by CO_3^{2-} in XMgAlCO$_3$ samples is very limited because of the difficulty of displacing a divalent anion by a monovalent and larger one.[33] Additionally the carbonate anion has a great affinity and specificity for the hydrotalcite interlayer position.[2] There is no relationship between TNP adsorption and AEC (Table 1), indicating that the AEC is not the determinant factor of the adsorption on these samples. The XRD pattern of the product corresponding to an isotherm point (50 mM) of Fig. 5a shows the presence of two phases: 3MgAl–TNP with d_{003} = 13.4 Å, and 3MgAlCO$_3$ with d_{003} = 7.8 Å as majority product (Fig. 6a). The coexistence of those two phases agrees with the maximum TNP adsorption obtained in the isotherm (17% of the AEC, Table 2).

The TNP adsorption isotherms on all calcined products were very similar (Fig. 5b). The maximum experimental adsorption measured was very much higher than in XMgAlCO$_3$ and practically the same for the three XMgAlCO$_3$500 samples (C_s = 4681, 4828 and 4698 μmol g^{-1}, for X = 2, 3 and 4, respectively). However, % of AEC exchange by TNP increases regularly with the increase of the Mg/Al ratio (Table 2). The reconstruction of the layered structure seems to be favored by the low layer charge. The X-ray diffraction pattern of the isotherm product (50 mM) shows two phases, 3MgAlCO$_3$ (d_{003} = 7.8 Å) and 3MgAl–TNP (d_{003} = 13.2 Å).

However, the X-ray diffraction pattern of the total anionic exchange (Fig. 6c) and reconstruction products (not shown) indicates the presence of a monophasic layered compound with the basal spacing of 3MgAl–TNP (d_{003} = 13.5 Å). The above results show that the sorbents (3MgAlCO$_3$ and 3MgAlCO$_3$500) produce a similar final compound after TNP adsorption. This fact was also confirmed by FT-IR spectroscopy of the product 3MgAl–TNP obtained by anion exchange from 3MgAlCO$_3$ and by reconstruction from 3MgAlCO$_3$500 shown in a previous paper.[35]

However, TNP adsorption by XMgAlCO$_3$ and its calcined products occurs by different ways, which can be represented by

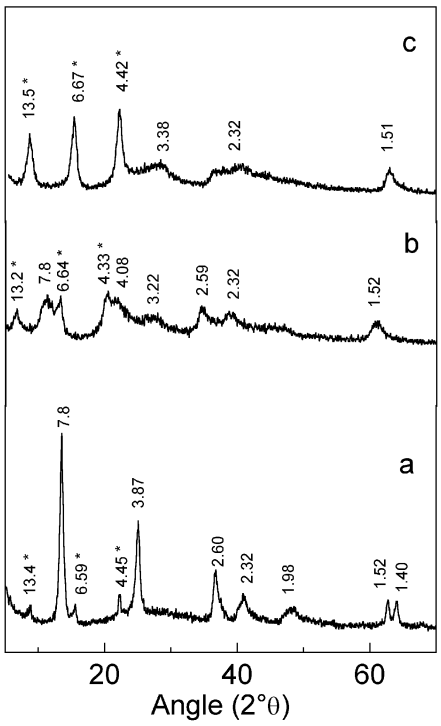

Fig. 6 X-Ray diffraction patterns of a) 3MgAlCO$_3$–TNP (isotherm plateau Fig. 5a), b) 3MgAlCO$_3$500–TNP (isotherm highest point Fig. 5b) and c) 3MgAl–TNP (total anionic exchange). (*) Diffraction lines (00l) corresponding to 3MgAl–TNP.

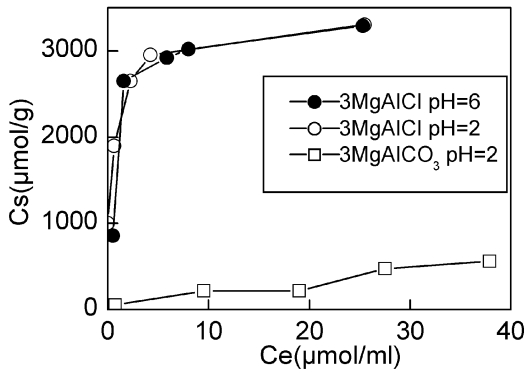

Fig. 7 Adsorption isotherms of TNP on different sorbents 3MgAlCl, pH = 2, 24 h; 3MgAlCl, pH = 6, 24 h and 3MgAlCO$_3$ pH = 2, 2 h. 0.05 g of sorbent per 10 ml of TNP in all cases.

eqn. (1) and (2) corresponding to the processes of anionic exchange and reconstruction respectively:

$$[Mg_{1-x}Al_x(OH)_2](CO_3)_{x/2}\cdot mH_2O + xTNP^- \rightarrow [Mg_{1-x}Al_x(OH)_2](TNP)_x\cdot mH_2O + x/2\ CO_3^{2-} \quad (1)$$

$$Mg_{1-x}Al_xO_{1+x/2} + (m+1+x/2)H_2O + xTNP^- \rightarrow [Mg_{1-x}Al_x(OH)_2](TNP)_x\cdot mH_2O + HO^- \quad (2)$$

These different ways could explain the different behavior with respect to the influence of the layer charge. In the first case [eqn. (1)] the adsorption is so low that it should occur only on the edges of the layers indicating that the large TNP anion is not able to diffuse through the interlayer to displace CO_3^{2-}. But according to eqn. (2) during reconstruction TNP anions are able to separate the layers collapsed during the heating, and in this case, the reconstruction must be easier when the layer charge is lower.[35]

MgAlCl system. *Influence of the interlayer anion.* Fig. 7 shows the adsorption isotherms of TNP on 3MgAlCl at two pH values (2 and 6, respectively). The adsorption isotherm of 3MgAlCO$_3$ is also included for comparison purposes. XMgAlCl samples show much higher adsorption than those corresponding to 3MgAlCO$_3$, varying between 59 and 104% of AEC for 2MgAlCl and 3MgAlCl respectively, and the adsorption is not significantly affected by the pH (Table 3). The Cl^- monovalent anions are easier to exchange for organic monovalent TNP anions than carbonate is. The same has been found by Sato and Okuwaki[33] with others organic anions. Carbonate anions have been shown to be difficult to displace from the interlayer of LDH in many exchange reactions[42]

Table 3 Langmuir model parameters for TNP adsorption and the corresponding %AEC of XMgAlCl (X = 2, 3 and 4) and 3MgFeCl hydrotalcites and their calcined products (XMgAlCl500 and 3MgFeCl500)[a]

Adsorbent	C_m/μmol g^{-1}	L	r^2	%AEC
2MgAlCl pH = 6	2380	0.61	0.99	59
3MgAlCl pH = 2	3333	2.72	0.99	100
3MgAlCl pH = 6	3448	1.03	0.99	>100
4MgAlCl pH = 6	1960	1.02	0.99	72
2MgAlCl500 pH = 4	2778	9.00	0.99	37
3MgAlCl500 pH = 4	3030	2.54	0.99	52
4MgAlCl500 pH = 4	3226	6.20	0.99	68
3MgFeCl pH = 6	1754	0.01	0.96	59
3MgFeCl500 pH = 4	1754	0.18	0.99	35

[a]AEC XMgAlCl500 = 7598, 5817 and 4714 μmol g^{-1} for X = 2, 3 and 4, respectively. AEC 3MgFeCl500 = 4981 μmol g^{-1}

and they require low pH experimental conditions to be displaced. However, LDH with the Cl^- as interlayer anion allows work at higher pH values (pH = 6), avoiding a partial dissolution of hydrotalcite, as occurred in the case of XMgAlCO$_3$ (pH = 2).

The adsorption process on XMgAlCl exhibits an L-type isotherm, indicating TNP is strongly attracted by the sorbent, mostly by ion–ion interactions between cations in the layer and TNP anions in the interlayer, which suggest that the layer charge may be important. This adsorption could be represented by eqn. (3) and it is completely displaced to the right as confirms the presence of a unique phase corresponding to XMgAl–TNP in the X-ray diagrams of the products (not shown).

$$[Mg_{1-x}Al_x(OH)_2]Cl_x\cdot mH_2O + xTNP^- \rightarrow [Mg_{1-x}Al_x(OH)_2](TNP)_x\cdot mH_2O + xCl^- \quad (3)$$

Influence of the layer charge (Mg/Al ratio). Fig. 8a and Table 3 show that the amount of TNP adsorbed increases with the layer charge increasing from 72% of AEC for 4MgAlCl to 104% for 3MgAlCl. The 2MgAlCl sample did not render the maximum adsorption as it should correspond to its highest layer charge. The FT-IR spectrum of that sample, with Mg/Al = 2 (not shown), indicates the presence of interlayer carbonate anions, indicating that it has not been possible to avoid the presence of this anion during the synthesis. Cl^- anions are not able to compensate for the high layer charge because of steric hindrance, and divalent interlayer anions of similar volume, such as CO_3^{2-}, are incorporated. However, FT-IR spectra of the samples with lower layer charge Mg/Al = 3 and 4 do not show the bands corresponding to the presence of CO_3^{2-} anion. Thus, the amount of TNP adsorbed by 2MgAlCl was not comparable with the amounts adsorbed by the samples 4MgAlCl and 3MgAlCl with only one interlayer species (Cl^-).

Comparing the higher adsorption capacity of 3MgAlCl with respect to 4MgAlCl, the high layer charge in the first case seems to favor the diffusion of TNP into the layer, displacing the Cl^- anion. The TNP adsorbed above AEC (104% in 3MgAlCl) could be due to additional adsorption of some neutral TNP molecules by aggregation, as has been observed for organic cationic clay minerals.[27]

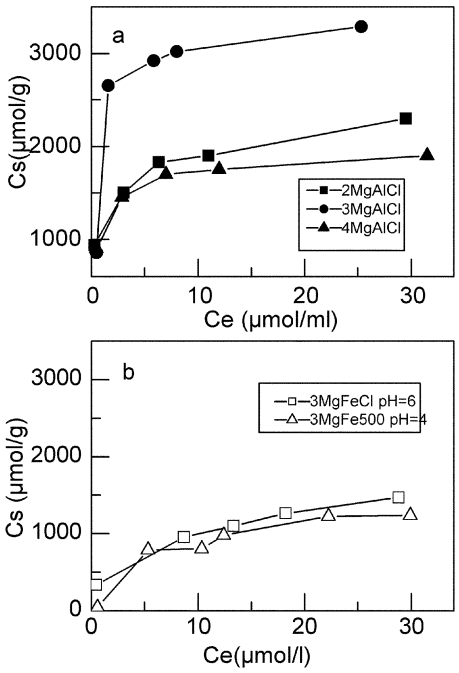

Fig. 8 Adsorption isotherms of TNP on different sorbents: a) XMgAlCl (0.05 g of sorbent per 10 ml of TNP, pH = 6, 24 h), and b) 3MgFeCl and 3MgFeCl500. (0.05 g of sorbent per 10 ml of TNP, 24 h).

In Table 3 are also included the TNP adsorption results when XMgAlCl500 are used as sorbents and as in the case of XMgAlCO$_3$500, the adsorption is not strongly affected by the layer charge, although in both cases the maximum adsorption is observed for the minimum layer charge, probably because the lower charge favors the layer separation and thus facilitates the hydrotalcite structure reconstruction. This different adsorption behavior of the original samples and its calcined products with the variation of the hydrotalcite layer charge could be related to the different adsorption mechanisms of these sorbents. In previous papers[32,35] we have indicated that the kinetics of TNP adsorption from solution by hydrotalcite and its calcined product at 500 °C are very different; the mechanisms of sorption found are consistent with an anion exchange process for hydrotalcite and by reconstruction of the layered structure for calcined hydrotalcite respectively. On the other hand, it could emphasize the much higher TNP adsorption on XMgAlCO$_3$500 than on XMgAlCl500 samples (Tables 2 and 3), probably related to the initial decomposition process, which in the case of XMgAlCO$_3$ is followed by CO_2 release. This CO_2 elimination does not occurs as a smooth diffusion in the interlayer, but through the holes in the crystal surface, which than appear as small spaced craters[43] as can be appreciated in Fig. 4b, thus favouring the interaction with TNP.

The XRD pattern of the adsorption product 3MgAlCl500–TNP in a point of the "plateau" of the isotherm (not shown) corresponds to a biphasic system similar to those shown in Fig. 6b for MgAlCO$_3$500.

These results confirm that the nature of the interlayer anion and charge density of the layers strongly affect the adsorption of TNP by the hydrotalcite-like compounds.

MgFeCl system. *Influence of the layer composition (Fe^{3+} vs. Al^{3+}).* 3MgFeCl was selected to study the influence of the presence in the layer of a trivalent transition cation on the adsorption process. The isotherm is of L-type, similar to that for 3MgAlCl (included in Fig. 8b), but with lower adsorption level. In the case of 3MgFeCl the maximum adsorption measured corresponds to only 59% of the AEC whereas in 3MgAlCl it reached 100% (Table 3).

In Fig. 9a and b, diffractograms for 3MgFeCl and for the complete anion exchange reaction product (0.5 g of hydrotalcite + 50 mM TNP) respectively are included. In the last case the diffraction peak of 13.6 Å confirms the presence of TNP as majority anion.[32] A small peak at 7.7 Å can be attributed to CO_3^{2-} anions, introduced in the interlayer on the exchange process due to the high affinity of hydrotalcite compounds for carbonate.[33] The XRD diagram of the isotherm product, Fig. 9c, shows the presence of two phases with trinitrophenolate anions (d_{003} = 13.6 Å) and chloride/carbonate anions (d_{003} = 7.8 Å) in the interlayer. The presence of the two phases agrees with measured values: about 50% of anionic exchange capacity saturated with TNP anions and the rest with Cl^- anions on different interlayers. The substitution of Al^{3+} by Fe^{3+} increases the effective charge on the layer which attracts strongly the chloride anions and probably constrains its displacement of the interlayer.

The TNP adsorption isotherm on the calcined product also shown in Fig. 8b is of L type. The calculated C_m value, 1754 μmol $^{-1}$g, is summarized in Table 3 and corresponds to only 35% of AEC. This value is very much lower than that expected and those observed in other calcined LDH (3MgAlCO$_3$500, >100% of AEC; 3MgAlCl500, 52% of AEC). The explanation is found in the XRD pattern of the calcination product 3MgFe500 (Fig. 10a) showing a biphasic material, where lines of the spinel phase $MgFe_2O_4$ and the MgO cubic phase are present. The XRD patterns of the product in the isotherm

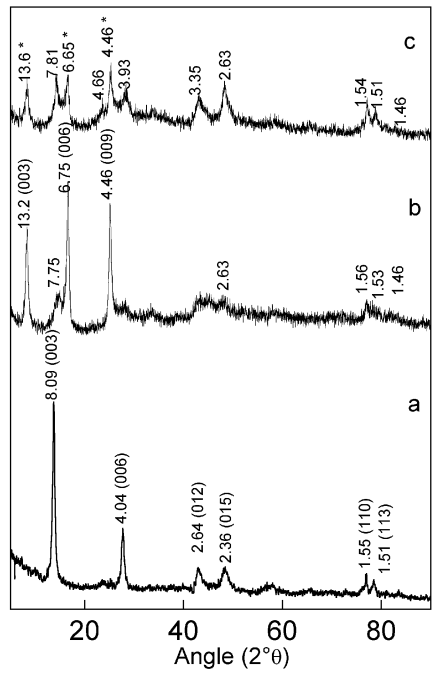

Fig. 9 X-Ray diffraction pattern of a) original 3MgFeCl, b) the anionic exchange product 3MgFeCl–TNP and c) the isotherm product in the "plateau" (Fig. 8a▲). (*) Diffraction lines (00l) corresponding to 3MgAl–TNP.

plateau (Fig. 10b) show changes in the relative intensity of the spinel lines with respect to the 3MgFe500 pattern: the intensity of the peak at 2.51 Å increases and those of the peaks at 2.09 and 1.48 Å decrease, additionally new lines corresponding to a layer phase with TNP as interlayer anion (d_{003} = 13.2 Å) are observed. The reconstruction process is not complete because of the high stability of the spinel phase[11] and only the portion of the calcined product corresponding to the MgO cubic phase is reconstructed. $MgFe_2O_4$ spinel structure and in general, spinels from hydrotalcite with transition metal cations in the layer are formed at lower temperature than $MgAl_2O_4$.[11,13]

The above results indicate that the nature of the cations present in the brucite layer will be a determining factor in the extension of the anionic exchange and reconstruction reactions in LDH and its calcined product. Further, the presence of Fe^{3+} ions on the layer determines the composition of the calcined product.

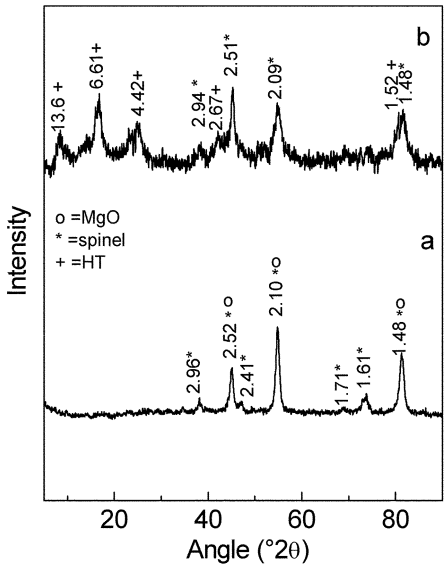

Fig. 10 X-Ray diffraction pattern of a) 3MgFe500 and b) the isotherm product MgFeCl500–TNP in the "plateau"(Fig. 8b).

Conclusions

The TNP adsorption on the MgAlCl system is much higher than on $MgAlCO_3$. The Cl^- anion is easily displaced from the interlayer up to reach 100% of the AEC, whereas CO_3^{2-} is difficult to displace by the phenolate anion. TNP adsorption by anionic exchange in the $MgAlCO_3$ system is very low and it is not possible to observe the influence of Mg/Al ratio (or layer charge), while in MgAlCl there is observed an increase of the TNP adsorption with an increase in the layer charge. The higher polarizing character of Fe^{3+} compared to that of Al^{3+}, makes the exchange reaction less favorable for the MgFeCl system. The phenol adsorption by reconstruction of the calcined product decreases as follows: $MgAlCO_3500$ > MgAlCl500 > MgFeCl500. The reconstruction is also favored with the layer charge decrease, because this process is constrained in the inner of the particle for the highest layer charge precursor. The higher TNP adsorption in $MgAlCO_3500$ systems than in MgAlCl500 ones, is related with to differences in the release of the anions (CO_3^{2-} and Cl^-) during the decomposition process. For MgFeCl500, the reconstruction is further restricted because the spinel develops (at lower temperature) and this phase does not revert to an interlayer structure. This fact causes adsorption by reconstruction in MgFeCl500 to be lower than expected and almost the same as in the original sample, MgFeCl, by anionic exchange.

Acknowledgement

This work has been partially supported by CICYT Project No. AMB96-0445-CO2-01 and Junta de Andalucía through Research Groups RNM-124 and FQM-214.

References

1 W. Jones and M. Chibwe, in *Pillared Layered Structures – Current Trends and Applications*, ed. I. V. Mitchell, Elsevier Applied Science, London and New York, 1990, p. 67.
2 F. Cavani, F. Trifiró and A. Vaccari, *Catal. Today*, 1991, **11**, 173.
3 A. de Roy, C. Forano and K. E. Malki, in *Expanded Clays and Other Microporous Solids*, eds. M. L. Occelli and H. E. Robson, Van Nostrand Reinhold, New York, 1992, p. 108.
4 V. Rives and M. A. Ulibarri, *Coord. Chem. Rev.*, 1999, **181**, 61.
5 D. L. Bish, *Bull. Mineral.*, 1980, **103**, 170.
6 H. Kopka, K. Beneke and G. Lagaly, *J. Colloid Interface Sci.*, 1988, **123**, 427.
7 M. Meyn, K. Beneke and G. Lagaly, *Inorg. Chem.*, 1990, **29**, 5201.
8 K. A. Carrado, A. Kostapapas and S. L. Suib, *Solid State Ionics*, 1988, **26**, 77.
9 W. T. Reichle, *Solid State Ionics.*, 1986, **22**, 135.
10 V. Rives, F. M. Labajos, M. A. Ulibarri and P. Malet, *Inorg. Chem.*, 1993, **32**, 5000.
11 F. Kooli, V. Rives and M. A. Ulibarri, *Inorg. Chem.*, 1995, **34**, 5114 and 5122.
12 C. Barriga, W. Jones, P. Malet, V. Rives and M. A. Ulibarri, *Inorg. Chem.*, 1998, **37**, 1812.
13 T. Sato, K. Kato, T. Endo and M. Shimada, *React. Solids*, 1986, **2**, 253.
14 F. Rey, V. Fornés and J. M. Rojo, *J. Chem. Soc., Faraday Trans.*, 1992, **88**, 2233.
15 T. Hibino, Y. Yamashita, K. Kosuge and A. Tsunashima, *Clays Clay Miner.*, 1995, **43**, 427.
16 M. Hudson, S. Carlino and C. Apperley, *J. Mater. Chem.*, 1995, **5**, 323.
17 K. Chibwe and W. Jones, *Chem. Mater.*, 1989, **1**, 489.
18 M. A. Ulibarri, F. M. Labajos, V. Rives, W. Kagunya, W. Jones and R. Trujillano, *Inorg. Chem.*, 1994, **33**, 2592.
19 J. Rocha, M. del Arco, V. Rives and M. A. Ulibarri, *J. Mater. Chem.*, 1999, **9**, 2499.
20 E. Kruissink, L. van Reijhen and J. R. H. Ross, *J. Chem. Soc., Faraday Trans*, 1981, **77**, 649.
21 W. Reichle, *J. Catal.*, 1985, **94**, 547.

22 F. Basile, L. Basini, M. D. Amore, G. Fornasari, A. Guarinoni, D. Matteuzzi, G. del Piero, F. Trifiró and A. Vaccari, *J. Catal.*, 1998, **173**, 247.
23 F. Medina Cabello, D. Tichit, B. Coq, A. Vaccari and N. Thy Dung, *J. Catal.*, 1997, **167**, 142.
24 A. Corma, S. Iborra, S. Miquel and J. Primo, *J. Catal.*, 1998, **173**, 315.
25 S. Carlino, *Chem. Br.*, 1997, September, 59.
26 M. C. Hermosîn and J. Cornejo, *Chemosphere*, 1992, **24**, 1493.
27 M. C. Hermosîn, P. Martín and J. Cornejo, *Environ. Sci. Technol.*, 1993, **27**, 2606.
28 L. J. Michot and T. J. Pinnavaia, *Clays Clay Miner.*, 1991, **39**, 634.
29 M. M. Mortland, S. Shaobai and S. A. Boyd, *Clays Clay Miner.*, 1986, **34**, 581.
30 R. C. Zielke and T. J. Pinnavaia, *Clays Clay Miner.*, 1988, **36**, 403.
31 M. J. Carrizosa, M. J. Calderon, M. C. Hermosîn and J. Cornejo, *Sci. Total. Environ*, 2000, **247**, 293.
32 M. A. Ulibarri, I. Pavlovic, M. C. Hermosîn and J. Cornejo, *Appl. Clay Sci.*, 1995, **10**, 131.
33 T. Sato and A. Okuwaki, *Solid State Ionics*, 1991, **45**, 43.
34 M. C. Hermosîn, I. Pavlovic, M. A. Ulibarri and J. Cornejo, *Water Res.*, 1996, **30**, 171.
35 I. Pavlovic, M. A. Ulibarri, M. C. Hermosîn and J. Cornejo, *Fresenius Environ. Bull.*, 1997, **6**, 266.
36 M. J. Sánchez Martín, M. V. Villa and M. S. Camazano, *Clays Clay Miner.*, 1999, **47**, 777.
37 C. C. Travis and E. Etnier, *J. Environ. Qual.*, 1981, **10**, 8.
38 S. Miyata, *Clays and Clay Miner.*, 1980, **28**, 50.
39 M. J. Hernández-Moreno, M. A. Ulibarri, J. L. Rendon and C. Serna, *Phys. Chem. Miner.*, 1985, **12**, 34.
40 F. M. Labajos, V. Rives and M. A. Ulibarri, *J. Mater. Sci*, 1992, **27**, 1546.
41 C. H. Giles, T. H. Mac Ewan, S. N. Nakhwa and D. Smith, *J. Chem. Soc.*, **1960**, 3973.
42 H. C. B. Hansen and C. B. Koch, *Clays Clay Miner.*, 1994, **42**, 170.
43 W. T. Reichle, S. Y. Kang and D. S. Everhardt, *J. Catal.*, 1986, **101**, 352.